IJNRD.ORG ISSN : 2456-4184
INTERNATIONAL JOURNAL OF NOVEL RESEARCH AND DEVELOPMENT (IJNRD) | IJNRD.ORG
An International Open Access, Peer-reviewed, Refereed Journal

EFFECT OF BROWNIAN MOTION AND THERMOPHOROSIS ON CONVECTIVE HEAT AND MASS TRANSFER FLOW OF A CASSON NANOFLUID PAST A STRETCHING CYLINDER WITH CHEMICAL REACTION AND IRREGULAR HEAT SOURCES

G. Kathyayani[1*], P Venkata Subrahmanyam[2],
[1]Professor, [2]Research Scholar
[1,2]Department of Applied Mathematics, Yogi Vemana University, Kadapa, A.P., India.

Abstract:
An attempt has been made to investigate combined impact of Brownian motion and thermophorosis of a Casson nanofluid past a stretching cylinder with chemical reaction and irregular heat sources. The system of ordinary differential equations is obtained by reducing the governing equation by the use of variables and boundary conditions. The Runge-Kutta fourth order method with the Shooting technique is used to approximate the numerical solutions. The effects of several relevant physical parameters on the velocity profiles and thermal profiles are displayed by using BVP4C conditions in *MATHEMATICA* software. It is found that an increasing Casson fluid parameter(β)/Brownian motion (Nb)/thermophorosis(Nt) produce an enhancement in the velocity, nanoparticle concentration and reduction in temperature in the boundary layer. Velocity(f'), temperature(θ) enhances nanoparticle concentration(ϕ) decreases with higher values of chemical reaction parameter(γ). The rate of mass transfer enhances in degenerating chemical reaction cases at the wall.

Keywords: Brownian motion, thermophoresis, Casson nanofluid, Stretching cylinder, Chemical reaction and non-uniform heat sources.

1. INTRODUCTION

Nanofluidic flow has received a lot of attention over the past twenty years due to its frequent applications in engineering and industry. In addition to learning more about the remarkable thermal characteristics of nanofluids, scientists and researchers hope to clarify the mechanisms underlying their thermal conductivity. Biosensors, agriculture, and pharmaceuticals could benefit from the combination of biotechnological mechanisms and nanofluids. The biotechnology sector uses a wide range of nanomaterials, such as nanowires, nanoparticles, nanofibers, and nanostructures. There is a steady demand for nanobiotechnology, and it is expected that these products will have a very bright future. In the same way, processes and biomedical devices cannot ignore the significance of nanofluids and microfluidics. Due to their dual magnetic and liquid characteristics, magnetic nanofluids are used in gratings, modulators, optical switches, and tunable fiber filters, among other numerous applications. Speaker magnetic nanoparticles and sink-float separation are essential in the treatment of cancer in medicine. Solar energy is the primary renewable energy source and it produces the least amount of environmental pollution. Direct solar energy can provide one with energy, water, and power. It is thought by researchers that introducing nanoparticles into the fluid can start the sunlight gathering process. Power production and distribution are two main

industrial operations that depend on the cooling and heating of fluids. The cooling system for high energy equipment needs to be improved every day (Choi et al[6], Kandasamy et al[14], Sheikholeslami[31], Wong et al [35]).

The discussion of gyrating Casson liquid flow with radiation effect was given by Archana et al. [2]. Previously Casson [4] has discussed the flow behavior of suspensions of pigments in oil and this is the initial article of Casson fluid. Kumar et al. [17] & Sadiq and Hayat [28] were scrutinized the mixed convective flow of Casson liquid via vertical plate with the impact of non-linear radiation. The Casson fluid flow of various fluids with several influencing effects through different surfaces was deliberated by some researchers (Archana et al. [1], Deepak Sarve et al.[7], Gireesha et al.[12], Kumar et al.[18]).

Many researchers have been interested in the applications of boundary layer flow and heat transfer over an exponentially extending cylinder in various fields, such as fiber technology, flow meter design, pipe and casting systems, etc. Lin and Shih [19], [20] were unable to obtain similar results when evaluating the laminar boundary layer and heat transfer along horizontally and vertically moving cylinders at constant velocity due to the cylinder's curvature effect. Wang [34] investigated the constant flow of an incompressible and viscous fluid outside of a stretching hollow cylinder in an ambient fluid at rest. Ishak et al. [13] examined the flow and heat transfer of an incompressible electrically conducted viscous fluid outside of a stretching cylinder in the presence of a continuous transverse magnetic field. Elbashbeshy et al. [10] studied the laminar boundary layer flow of an incompressible viscous fluid along a stretching horizontal cylinder immersed in a porous media in the presence of a heat source or sink with suction/injection.

Applications of Casson fluid flow in cylindrical shape in blood flow are significant. Fredrickson [11] investigated a casson fluid's passage via a tube. Researchers Nagarani and Sarojamma [23] looked into how body acceleration affected blood flowing via a stenosed artery modelled as a Casson fluid. Blood was modeled as a Casson fluid and the blood flow through a stenosed catheterized artery was examined by Sarojamma et al. [30]. Tamoor et al. [32] have studied the hydromagnetic flow of Casson fluid along a stretching cylinder.

The impact of non-uniform heat sink or source has numerous uses in the medical field as well as numerous technical endeavors, such as the cooling of metal sheets, the extraction of crude oil, and thrust bearing operations. Uneven heat parameters were covered by Tawade et al. [33] in relation to time - dependent thin film motion in magnetohydrodynamics when radiative heat flow appeared. The heat transfer properties on the time-dependent motion of an electrically followed Casson and Williamson shear-thickening nanoliquids due to plate stretching were described by Zuhra et al. [37]. Patil et al. [25] examined the effects of Soret and Dufouron MHD driven convective motion on an exponentially stretched sheet with variable heat values. The governing equations are numerically solved using the quasi-linearization technique. It was determined that increasing the values of the irregular heat raise/fall parameters lowers the local Nusselt number. A few days ago, Ramadevi et al. [27] investigated the heat and mass transport properties of an electrically conducting flow of a shear-thickening fluid across a coagulated surface. Dogonchi et al. [8] looked at the impact of Lorentz force on free convective flow caused by cylinder stretching. The effects of ohmic heat and different fluid properties on the time-dependent flow of a shear-thickening liquid across a stretched sheet in the presence of drag force were studied by Mahmoud and Megahed [21]. Khan et al. [15] investigated the flow and heat transmission characteristics of a second-grade shear-thickening liquid produced by stretching a cylinder with temperature-dependent thermal conductivity.

Density, specific heat, Viscosity and thermal conductivity are the primary thermophysical variables that determine a nanofluid's heat transmission characteristics. Many studies have looked into the rheology of nanofluid in order to model the viscosity of the fluid. However, scientists thought that nanofluid behaved like a Newtonian fluid (Penkavova et al[26], Namburua et al. [24] others observed non – Newtonian behaviour (Duan et al[9], Kulkarni et al[16]). Rheology of nanofluids was studied as part of the International Nanofluid Property Benchmark Exercise (INPBE). The results showed that nanofluids exhibit both Newtonian and non-Newtonian behavior. Chen et al. [5] state that the viscosity of the base fluid, the volume fraction, and the shear rate all influence how shear thinning nanofluids are. When the volume fraction was less than 0.05 at low shear rates, shear thinning was observed; when the volume fraction was less than 0.001, no shear thinning behavior was evident. All shear rate values exhibit shear thinning, nevertheless, when the volume fraction above 0.05.

Sarojamma and Vendabai [29] have examined the boundary layer flow of a casson nanofluid over a vertical exponentially extending cylinder in the presence of an internal heat generation/absorption and a transverse magnetic field.

In this work, we investigate the effects of magnetic field and a non-uniform heat source on the hydromagnetic boundary layer flow of a Casson nanofluid along a vertical exponentially stretching cylinder. The governing equations are converted into a system of coupled nonlinear ODEs by a similarity transformation. These equations are solved using Runge–Kutta fourth order method and the shooting approach. The graphical representation of the various parameter variations is shown.

2. FORMULATION OF THE PROBLEM:

We study the Casson fluid's boundary layer flow undergoing natural convection past a vertically stretched circular cylinder of radius 'a'. It is assumed that the cylinder is stretched exponentially with a velocity of U_∞ in the radial direction. The symbol T_w indicates the temperature at the cylinder's surface and the uniform ambient temperature as T_∞. When there is assisting flow the quantity $T_w - T_\infty > 0$, while it is taken to be negative for the opposing flow respectively (Fig.1).

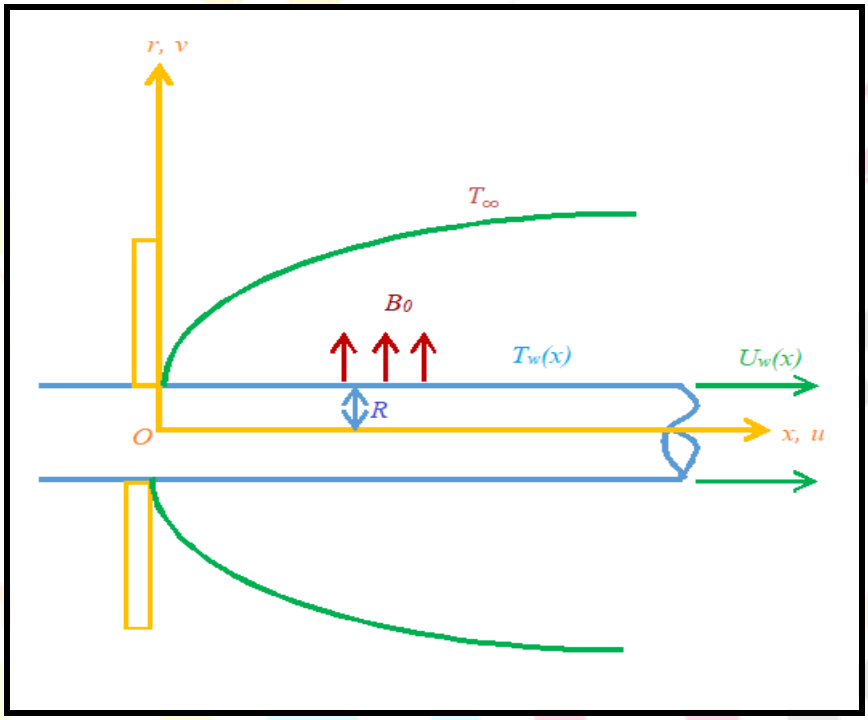

Fig. 1 : physical model

Under Boussinesq and Rosseland approximations the continuity, momentum, energy and nanoparticle concentration equations are (Buongiarno[3]):

$$\frac{\partial u}{\partial r}+\frac{u}{r}+\frac{\partial w}{\partial z}=0 \tag{1}$$

$$u\frac{\partial w}{\partial r}+w\frac{\partial w}{\partial z}=-\frac{1}{\rho}\frac{\partial p}{\partial z}+\nu(1+\frac{1}{\beta})(\frac{\partial^2 w}{\partial r^2}+\frac{1}{r}\frac{\partial w}{\partial r})+\beta_T g(T-T_\infty)(1-\phi_\infty)+$$
$$+\frac{1}{\rho}(\rho_\infty-\rho)(\phi-\phi_\infty)-(\frac{\sigma B_o^2}{\rho})w \tag{2}$$

$$u\frac{\partial T}{\partial r}+w\frac{\partial T}{\partial z}=(\frac{k_f}{\rho C_p}+\frac{16\sigma^* T_\infty^3}{\rho C_p \beta_R})(\frac{\partial^2 T}{\partial r^2}+\frac{1}{r}\frac{\partial T}{\partial r})+\frac{(\rho C_p)^*}{(\rho C_p)}(D_T\frac{\partial T}{\partial r}\frac{\partial \phi}{\partial r}+\frac{D_T}{T_\infty}(\frac{\partial T}{\partial z})^2)+\frac{q'''}{\rho C_p} \tag{3}$$

$$u\frac{\partial \phi}{\partial r}+w\frac{\partial \phi}{\partial z}=(D_B)(\frac{\partial^2 \phi}{\partial r^2}+\frac{1}{r}\frac{\partial \phi}{\partial r})+\frac{D_T}{T_\infty}(\frac{\partial^2 T}{\partial r^2}+\frac{1}{r}\frac{\partial T}{\partial r})-k(\phi-\phi_\infty) \tag{4}$$

where (u,w) are velocity components along (r,z) directions, $\rho,\rho_\infty,\nu,p,g,\beta,\beta_T,\sigma^*,\beta_R,T,\phi,T_w,\phi_w,T_\infty,\phi_\infty,(\rho C_p)^*,(\rho C_p),\sigma,B_o,q''',C_p$, D_B, D_T, kc, are density of fluid,

density at infinity, kinematic viscosity, pressure, gravitational acceleration along z-direction, coefficient of Casson fluid, coefficient of, thermal expansion, temperature, nanoconcentration of the fluid, wall temperature, concentration, ambient temperature, concentration, heat capacity of base fluid, effective heat capacity of the nanoparticle material, electrical conductivity, magnetic field intensity, rate of internal heat generation (>0) or absorption(<0)coefficient, Brownian diffusion coefficient, thermophoresis diffusion coefficient, chemical reaction coefficient, specific heat at constant pressure respectively. A uniform magnetic field of intensity B0 is assumed to acts in the radial direction.

To model the internal heat generation or absorption term q''' , the following equation is used:

$$q''' = \frac{k_f U_w(z)}{a\nu}[A_{11}^{'}(T_w - T_\infty) f' + B_{11}^{'}(T - T_\infty)] \qquad (5)$$

Where $A_{11}^{'}$ and $B_{11}^{'}$ are the coefficient of space and temperature dependent heat source/sink respectively. Observe that the cases $A_{11}^{'} > 0,\ B_{11}^{'} > 0$ refers to internal heat generation while $A_{11}^{'} < 0,\ B_{11}^{'} < 0$ refers to internal heat absorption. Also we take $U_w(z) = 2ak_f \exp(\frac{z}{a})$($k$ is the dimensiona l constant) as the velocity of the fluid at the cylinder's surface.

The similarity variables are introduced as follows:

$$\eta = \frac{r^2}{a^2}, u = -\frac{1}{z}U_w \frac{f(\eta)}{\sqrt{\eta}}, w = U_w f'(\eta), \theta = \frac{T - T_\infty}{T_w - T_\infty}, C = \frac{\phi - \phi_\infty}{\phi_w - \phi_\infty} \qquad (6)$$

Where the characteristic temperature and difference in nanoconcentration are computed from the relations $T_w - T_\infty = c\exp(\frac{z}{a})$ *and* $\phi_w - \phi_\infty = \exp(\frac{z}{a})$. As a result of transformation equation (6), equations (2)-(4) are reduced to

$$(1+\frac{1}{\beta})(\eta f''' + f'') + \mathrm{Re}(ff'' + (f')^2) + \mathrm{Re}\, Gr(1-\phi_\infty)(\theta + NrC) - M^2 f' = 0 \qquad (7)$$

$$\eta\theta'' + \theta' + \mathrm{Re}\,\mathrm{Pr}(f\theta' - f'\theta) + \eta\theta'(Nb\theta' C' + Nt(\theta')^2) + \mathrm{Re}(A_{11} f' + B_{11}\theta) = 0 \qquad (8)$$

$$\eta C'' + C' + (\frac{Nt}{Nb})(\eta\theta'' + \theta') + \mathrm{Re}(fC' - f'C) - Le\gamma C = 0 \qquad (9)$$

where $Gr = \frac{\beta_T g a(T_w - T_\infty)}{U_w^2}, \mathrm{Pr} = \frac{\mu C_p}{k_f}, Le = \frac{\nu}{D_B}, Nr = \frac{(\rho_{f\infty} - \rho)(\phi_w - \phi_\infty)}{\rho\beta_T(T_w - T_\infty)(1-\phi_\infty)},$

$$Nb = \frac{(\rho C_p)_{nf} D_B(\phi_w - \phi_\infty)}{\rho C_p \alpha}, Nt = \frac{(\rho C_p)_{nf} D_T(T_w - T_\infty)}{\rho C_p \alpha T_\infty}, \mathrm{Re} = \frac{aU}{4\nu}, \alpha = \frac{k_f}{\rho C_P}, \gamma = \frac{kc}{a}$$

are the Grashof number, Prandtl number, Lewis number, buoyancy ratio, Brownian motion parameter, thermophoresis parameter, Reynolds number, thermal diffusivity, chemical reaction parameter respectively.

The following are the transformed boundary conditions:

$$\begin{aligned} &f(1) = 0,\ f'(1) = 1,\ f' \to \infty, as\ \eta \to \infty \\ &\theta(1) = 1, \theta \to 0, as\ \eta \to \infty \\ &C(1) = 1, C \to 0, as\ \eta \to \infty \end{aligned} \qquad (10)$$

Shear stress at the surface τ_w, the skin friction C_f, local Nusselt number Nux, the local Sherwood number Shx are important physical quantities given by

$$\tau_w = (w_{rz})_{r=a,}\ q_w = -(k_f(\frac{\partial T}{\partial z})_{r=q}, m_w = D_B(\frac{\partial \phi}{\partial z})_{r=a}$$

$$C_f = \frac{\tau_w}{\rho U_w^2}, Nux = \frac{ae^{z/a} q_w}{k_f(T_w - T_\infty)}, Shx = \frac{e^{z/a} m_w}{D_B(\phi_w - \phi_\infty)} \qquad (11)$$

Where q_w refers to heat flux and m_w refers to mass flux at the surface of the cylinder.

The fourth-order Runge-Kutta technique and the shooting method are used in this study to get numerical solutions.

3. COMPARISON

The Skin Friction Coefficient and Local Nusselt Number are compared numerically in the absence of M, A11, B11, γ

Table: 1

$f''(1)$	Malik et al. [22]	Sarojamma and Vendabai [29]	**Present Results**	Malik et al. [22]	Sarojamma and Vendabai [29]	**Present Results**
λ/β	0.1			0.3		
0.2	0.8494	0.849336	**0.849330**	1.1283	1.128340	**1.128345**
0.4	0.7873	0.783830	**0.783831**	0.9860	0.986953	**0.986947**
0.6	0.7263	0.726417	**0.726418**	0.8490	0.849073	**0.849088**
0.8	0.6662	0.666156	**0.666158**	0.7162	0.716398	**0.716402**
1.0	0.6070	0607086	**0.607089**	0.5869	0.586522	**0.586524**

Table : 2

$-\theta'(1)$	Malik et al. [22]	Sarojamma and Vendabai [29]	**Present Results**	Malik et al. [22]	Sarojamma and Vendabai [29]	**Present Results**
Pr/Re	0.1			0.2		
1	0.2442	0.244205	**0.244209**	0.3094	0.309400	**0.309405**
3	0.3826	0.382587	**0.382592**	0.5627	0.562756	**0.562759**
5	0.5118	0.511778	**0.511784**	0.7844	0.784403	**0.784406**
7	0.6327	0.632698	**0.632701**	0.9814	0871388	**0.871392**
15	1.0499	1.049939	**1.049942**	0.6121	1.612127	**1.612129**

4. RESULTS AND DISCUSSION:

In this study, we explore the combined influence of activation energy and variable viscosity on hydromagnetic convective heat and mass transfer flows of a Casson nanofluid past a stretching cylinder. We have solved the non-linear equations regulating the flow, heat and mass transfer of the Casson fluid flow using the Runge-Kutta fourth order with shooting technique. This investigation aims to comprehend the impact of several parameters, including the Grashof number (G), Casson parameter(β), magnetic parameter (M), buoyancy ratio (Nr), thermophoresis parameter(Nt), Brownian motion parameter(Nb), Prandtl number(Pr), Lewis number(Le), heat source parameters (A11,B11), Reynolds number(Re) on velocities, nanoparticle concentration and temperature are graphically represented. By comparing the results with those of Sarojamma et al [29] in the absence of a magnetic field (M=0), a space-dependent heat source (A11=0), and a temperature – dependent heat source (B11=0), and chemical reaction parameter(η=0), discovered that there is good agreement between the outcomes.

The fluctuation of temperature, velocity, and nanoparticle concentration with Grashof number (G) and magnetic parameter (M) is shown in Figs. 2a–2c. A rise in G lead to a reduction in temperature and an increase in axial velocity and nanoparticle concentration. Greater temperature, lower velocity, and a concentration of nanoparticles are associated with stronger magnetic fields. The hydrodynamic boundary layer shrinks as a result of the Lorentz force acting as a resistive force (figs. 2a-2c).

Figs. 3a-3d demonstrates the impact of the Casson parameter (β) and buoyancy ratio (Nr) on flow variables. It has been noted that when β rises, velocity and nanoparticle concentration increase and temperature drops. As the buoyancy forces are applied in the same direction, we observe that temperature falls with respect to buoyancy ratio (Nr), but velocity and nanoparticle concentration increase when the molecular buoyancy force dominates over the thermal buoyancy force.

Figures 4a–4c show how flow variables are affected by the thermophoresis parameter (Nt) and the Brownian motion parameter (Nb). It has been reported that Brownian motion (Nb), which promotes micro mixing, is accountable for improving the nanofluid's thermal conductivity. As a result, we can anticipate that the temperature will rise in proportion to Brownian motion. Clearly, higher Nb values are associated with higher temperature and velocity in the boundary layer. The flow zone experiences a reduction in the concentration of nanoparticles. Temperature and velocity increase when the thermophoresis parameter (Nt) increases, yet the concentration of nanoparticles in the flow zone decreases.

The impact of space dependent heat source (A11) on flow variables can be seen from figs.5a-5c. It is clear that rising A11 values lead to improvements in the fluid's temperature, velocity, and decrease in the concentration of nanoparticles.This might be explained by the fact that the existence of a heat source (A11>0) would produce energy and cause the temperature to rise. However, the converse happens

when A11<0 (heat sink) is used, which results in the fluid cooling. Consequently, the thickness of the thermal boundary layer diminishes.

The impact of temperature dependent heat generating source(B11>0)/heat absorbing source (B11<0) on flow variables can be seen from figs,6a-6c. It is discovered that when there is a heat-generating source (B11>0), the boundary layer's temperature, velocity, and nanoparticle concentration all rise. Conversely, when there is a heat-absorbing source, the boundary layer's nanoparticle concentration, temperature , velocity all decrease.

The effects of Reynolds number (Re) and chemical reaction parameter (γ) on temperature, velocity and nanoconcentration are shown in Figs. 7a–7c. Increase in Re increases velocity and nano particle concentration and depreciate the temperature. Also we found that temperature, velocity reduce and nanoparticle concentration experience reduction in the degenerating chemical reaction case.

Figs.8a-8c represent the effect of Prandtl number(Pr) and Lewis number(Le) on flow variables. With reference to Pr, we find that rising values of Pr makes a reduction in nanoparticle concentration, temperature, velocity. Since Pr is the ratio between viscous diffusion rate and thermal diffusion rate, increased Pr values correspond to reduced thermal diffusivity, causing the thermal boundary layer to shrink due to a decrease in energy ability. As Lewis number(Le) increases, momentum, solid boundary layers become thicker while thermal boundary layers become thinner.

The variation of Nusselt number(Nu), Sherwood number(Sh) and skin friction (Cf) on the stretching cylinder for different parametric variations is shown in table.3. Increase in G or Reynolds number (Re) or buoyancy ratio(Nr), reduces skin friction, Sherwood number(Sh) and enhances Nusselt number on the wall. Greater the Lorentz force, larger the skin friction, Sherwood number, smaller the heat transfer rate on η=0. Higher values of Casson parameter (β) decays skin friction, Sherwood number and grows heat transfer rate on the wall. Higher values of Brownian motion(Nb)/thermophoresis parameter (Nt) leads to growth in skin friction, Nusselt number and enhances in Nusselt number on η=0. Increasing the chemical parameter (γ), improves the Sherwood number where as the skin friction and Nusselt number reduces. An increasing A11>0 and B11>0 leads to a reduction in skin friction while it enhances with A11<0 and reduces B11<0. As the strength of the spatially and temperature-dependent heat source increases, the heat transfer rate decreases and increases
with that spatial/temperature dependent heat sink on the wall. The Sherwood number grow with increasing A11>0, B11>0 and decays with A11<0, B11<0. Sh grows with Lewis(Le) number on η=0. Lesser the thermal diffusivity larger the skin friction, heat transfer rate and smaller the mass transfer rate on the wall.

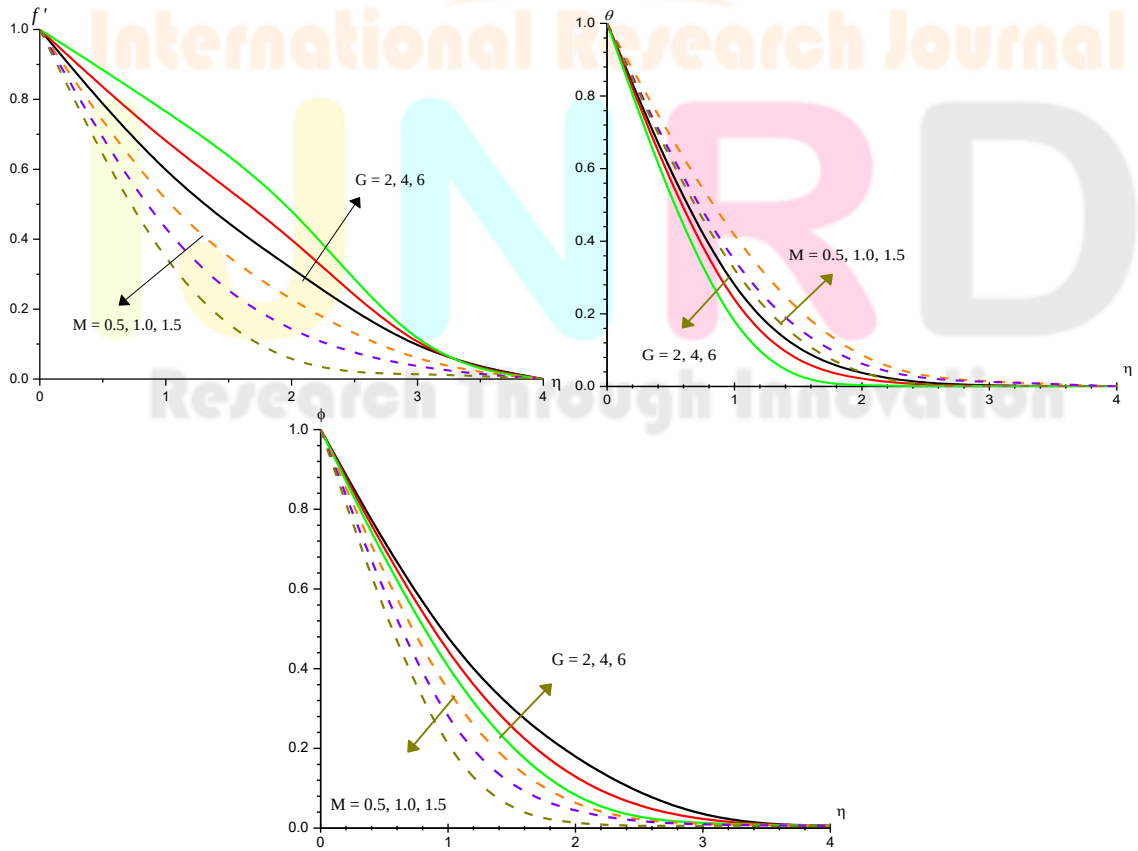

Fig.2.Variation of [a] velocity(f'), [b] Temperature(θ), [c] Nano-Concentration(ϕ) with G and M
β=0.25, Nr=0.5, Nb=0.1, Nt=0.2, A11=0.1, B11=0.1, Re=0.3, γ=0.5, Le=1, Pr=0.71

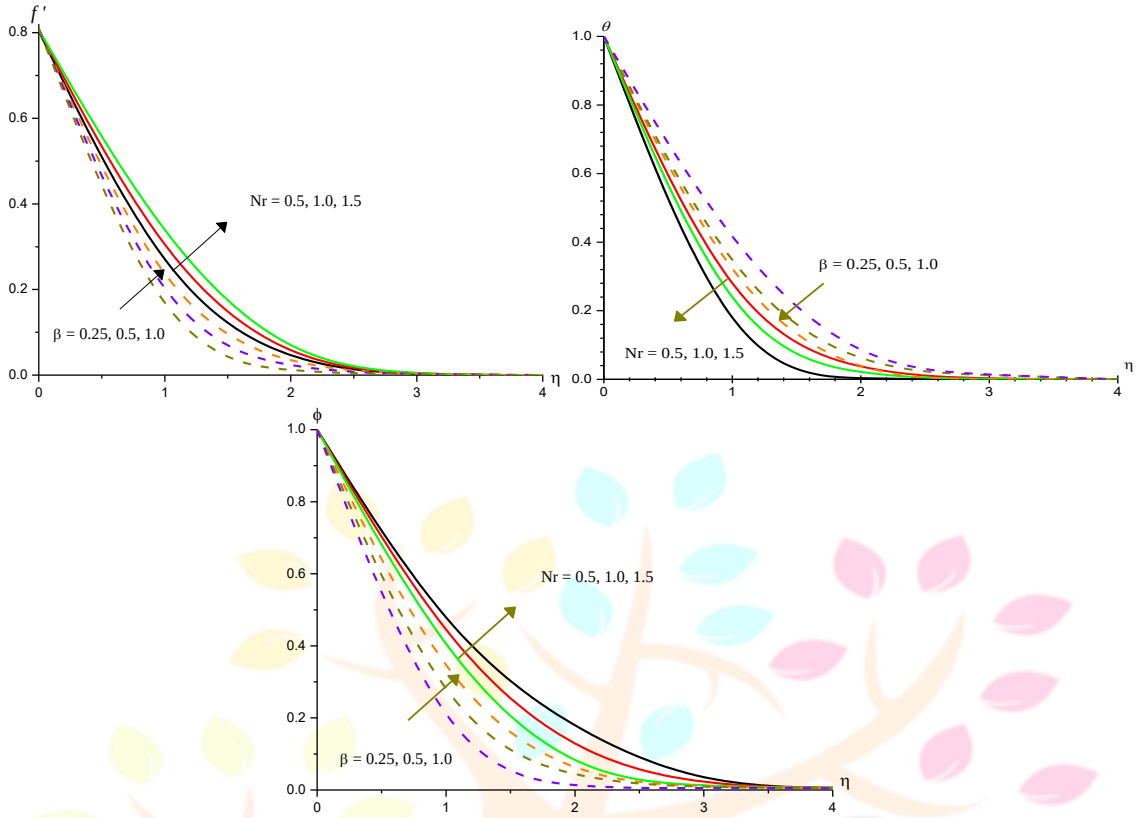

Fig.3.Variation of [a] velocity(f'), [b] Temperature(θ), [c] Nano-Concentration(ϕ) with β and Nr
G=2, M=0.5, Nb=0.1, Nt=0.2, A11=0.1, B11=0.1, Re=0.3, γ=0.5, Le=1, Pr=0.71

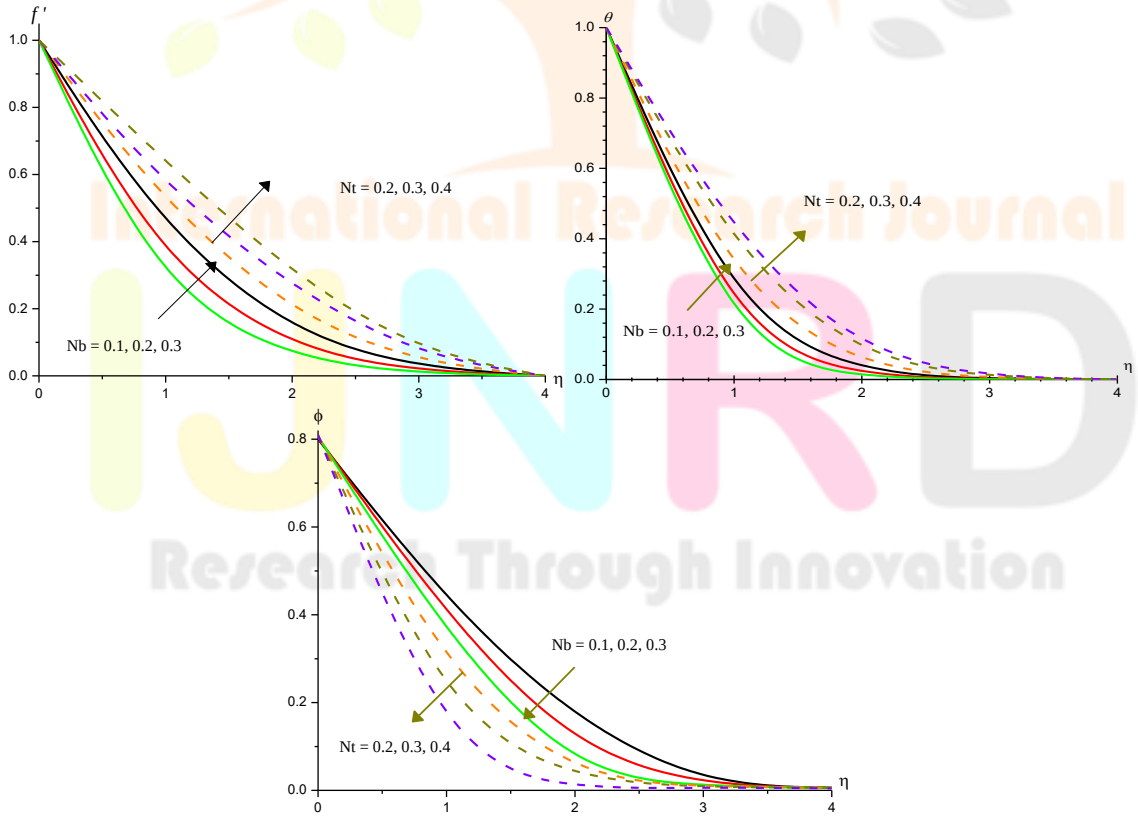

Fig.4.Variation of [a] velocity(f'), [b] Temperature(θ), [c] Nano-Concentration(ϕ) with Nb and Nt
G=2, M=0.5, β=0.25, Nr=0.5, A11=0.1, B11=0.1, Re=0.3, γ=0.5, Le=1, Pr=0.71

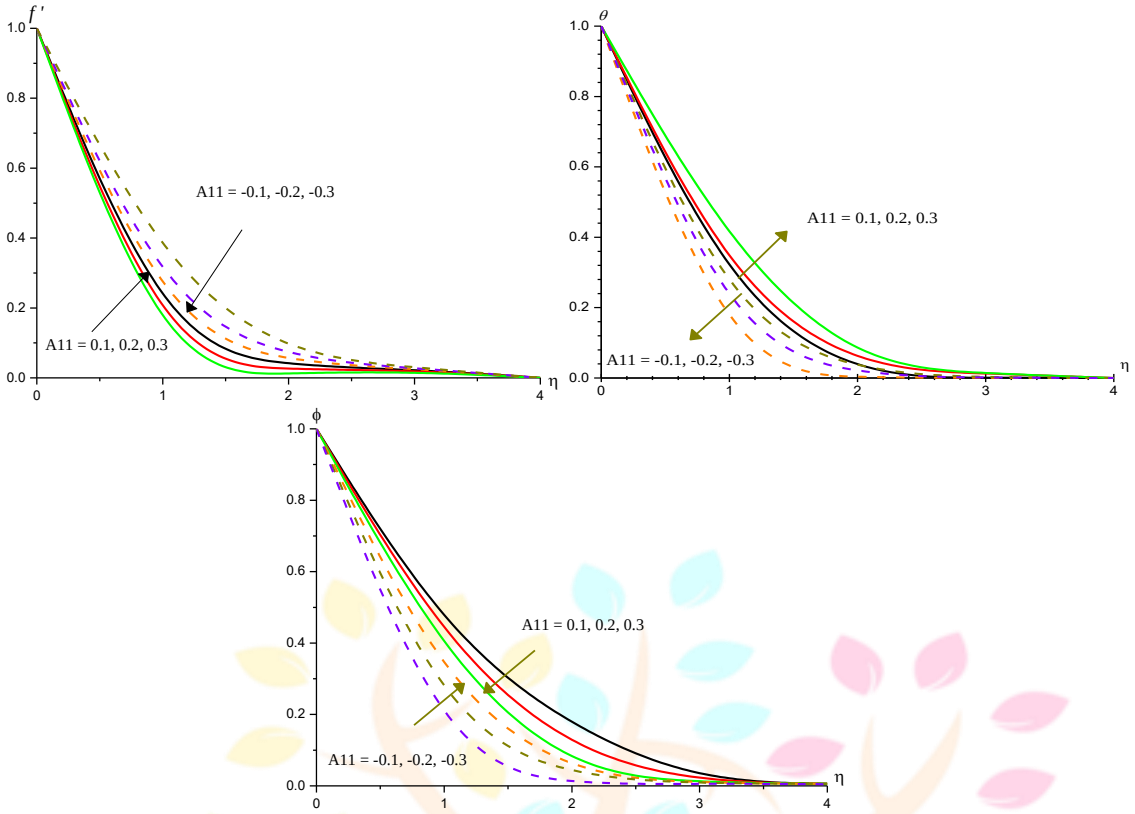

Fig.5.Variation of [a] velocity(f'), [b] Temperature(θ), [c] Nano-Concentration(ϕ) with A11 (±)
G=2, M=0.5, β=0.25, Nr=0.5, Nb=0.1, Nt=0.2, B11=0.1, Re=0.3, γ=0.5, Le=1, Pr=0.71

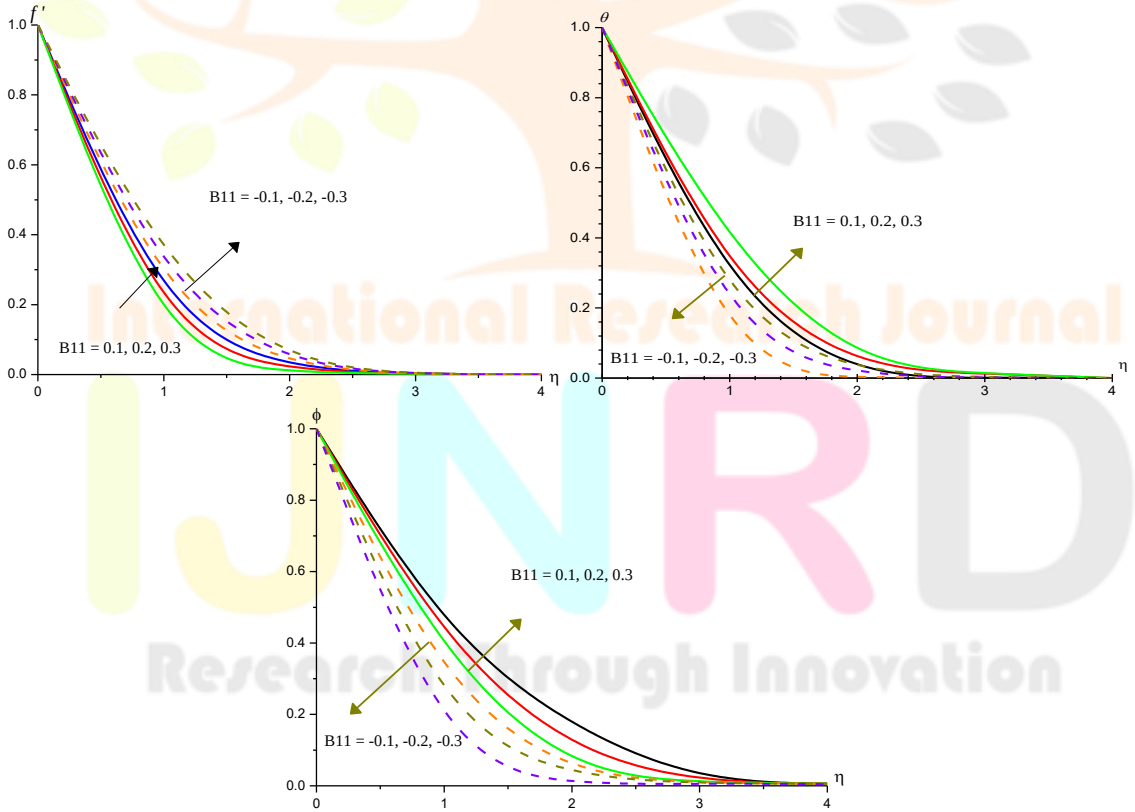

Fig.6.Variation of [a] velocity(f'), [b] Temperature(θ), [c] Nano-Concentration(ϕ) with B11 (±)
G=2, M=0.5, β=0.25, Nr=0.5, Nb=0.1, Nt=0.2, A11=0.1, Re=0.3, γ=0.5, Le=1, Pr=0.71

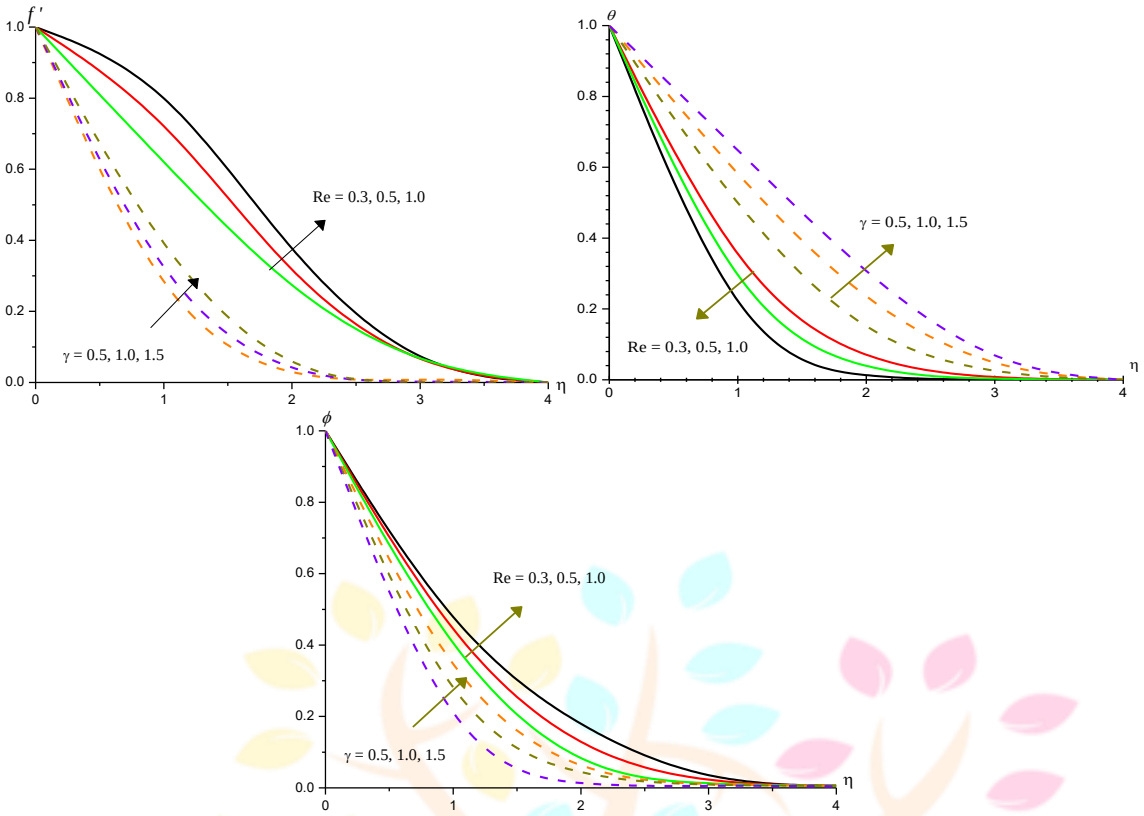

Fig.7.Variation of [a] velocity(f'), [b] Temperature(θ), [c] Nano-Concentration(ϕ) with Re and γ
G=2, M=0.5, β=0.25, Nr=0.5, Nb=0.1, Nt=0.2, A11=0.1, B11=0.1, Le=1, Pr=0.71

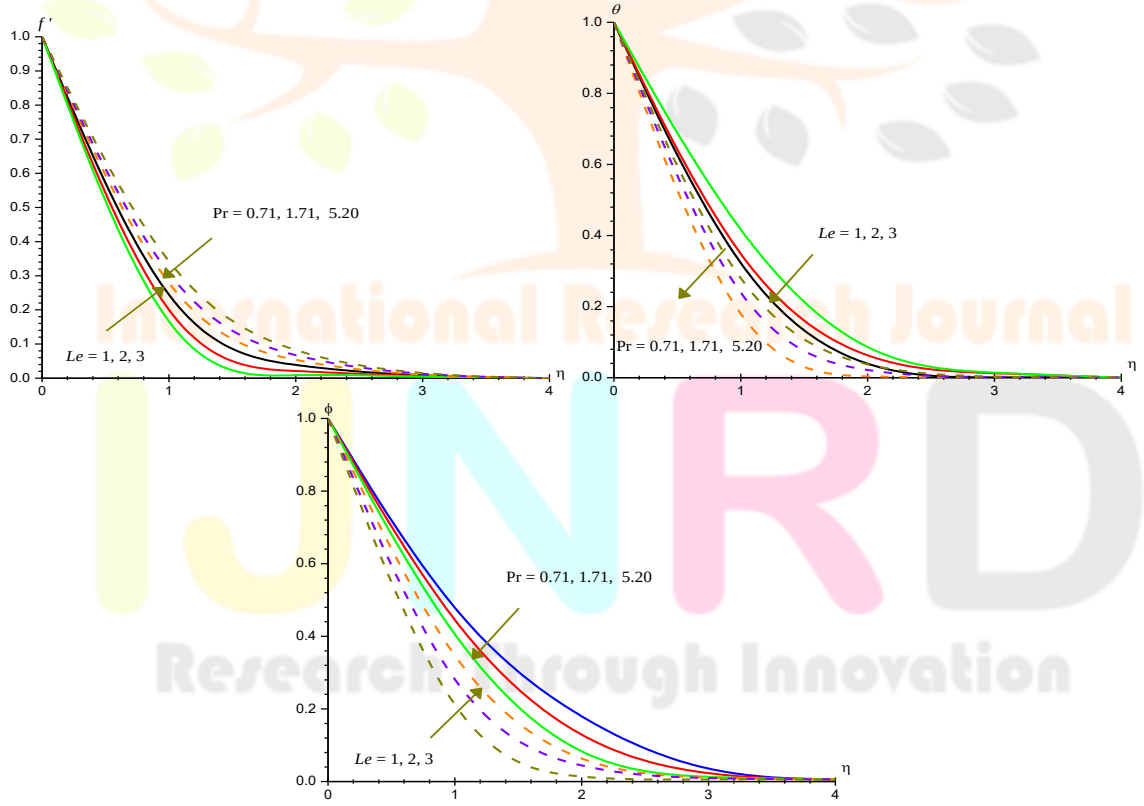

Fig.8.Variation of [a] velocity(f'), [b] Temperature(θ), [c] Nano-Concentration(ϕ) with Le and Pr
G=2, M=0.5, β=0.25, Nr=0.5, Nb=0.1, Nt=0.2, A11=0.1, B11=0.1, Re=0.3, γ=0.5

Table – 3 : Skin Friction (C_f), Nusslet number (Nu) and Sherwood Number (Sh) at η = 0

Parameter		Cf(1)	Nu(1)	Sh(1)		Parameter		Cf(1)	Nu(1)	Sh(1)
G	2	-0.614091	0.680323	1.50149		Re	0.3	-0.614091	0.680323	1.50149
	4	-0.603525	0.682469	1.47474			0.7	-0.607796	0.820447	1.49586
	6	-0.593754	0.683474	1.46135			1.0	-0.602792	0.929788	1.46304

M	0.5	-0.636939	0.678817	1.50174		γ	0.5	-0.626631	0.664662	1.86179
	1.0	-0.649944	0.678083	1.50183			1.0	-0.615093	0.648153	2.29285
	1.5	-0.683718	0.675991	1.50215			1.5	-0.612913	0.622845	2.93943
Nr	0.25	-0.614091	0.680323	1.50149		Pr	0.71	-0.614091	0.680323	1.50149
	0.5	-0.613523	0.681893	1.47482			1.71	-0.614108	0.736445	1.42274
	1.0	-0.613194	0.682356	1.45149			6.2	-0.614235	0.871262	1.39371
β	0.2	-0.626238	0.679286	1.50173		Le	1	-0.624809	0.795781	1.59303
	0.4	-0.608466	0.680375	1.50157			2	-0.614216	0.677345	1.67951
	0.6	-0.606447	0.680393	1.50164			3	-0.614314	0.672782	1.83888
Nb	0.1	-0.614091	0.680323	1.50149		Nt	0.2	-0.625014	0.586477	1.62694
	0.2	-0.614025	0.647794	1.51632			0.3	-0.613992	0.504261	1.90295
	0.3	-0.614011	0.620808	1.55635			0.5	-0.612066	0.423993	2.32904
A11	-0.1	-0.614091	0.680323	1.50149		B11	-0.1	-0.614091	0.680323	1.50149
	-0.2	-0.614096	0.726628	1.43213			-0.2	-0.614089	0.723821	1.43479
	-0.3	-0.614197	0.767442	1.42028			-0.3	-0.614184	0.760505	1.42662
	0.1	-0.624933	0.637254	1.54109			0.1	-0.624918	0.637965	1.54044
	0.2	-0.613986	0.593122	1.58278			0.2	-0.613986	0.593197	1.58271
	0.3	-0.613934	0.550556	1.62246			0.3	-0.613930	0.547736	1.62504

5. CONCLUSION:

In this paper, we study the boundary layer flow of Casson nanofluid over a stretching cylinder with irregular heat source under the effect of a transverse magnetic field. The model considers the combined influence of irregular heat sources, yield stress, Brownian motion and thermophorosis on the flow phenomenon. An illustration of how different physical parameters affect the flow variables is shown. There were significant findings in the study, which are summarized below, and may be relevant to future research in this field.

- The convection parameter(G)/buoyancy ratio(Nr)/Casson fluid parameter(β) produce an enhancement in the velocity(f'), nanoparticle concentration(ϕ) and reduction in temperature(θ) in the boundary layer.
- An increase in thermophoresis(Nt) and Brownian motion (Nb), enhances f' and θ and reduces ϕ.
- f', θ enhances ϕ decreases with rising values of chemical reaction parameter(γ), Sh enhances in degenerating chemical reaction cases at the wall. f', θ experience enhancement with spatial/temperature dependent heat source while ϕ reduces with A11>0, increases with B11>0.Nu decays and Sh grows with increase in A11 and B11 at η=0.
- The Lewis number(Le) enhances the ϕ and grows the mass transfer rate at the wall. Increasing Prandtl number(Pr) leads to depreciation in f', θ and ϕ. The C_f, Nu grow, Sh decays on the wall η=0 with higher values of Pr.

6.REFERENCES

[1]. Archana M., Gireesha B. J., Prasannakumara B. C.,Triple diffusive flow of Casson nanofluid with buoyancy forces and nonlinear thermal radiation over a horizontal plate, Archives of Thermodynamics, 40(1), (2019), 49-69.

[2]. Archana M., Gireesha B. J., Prasannakumaraand B. C., Gorla R.S.R., Influence of nonlinear thermal radiation on rotating flow of Casson nanofluid, 7(2), (2017), 91-101.

[3]. Buongiarno, J. "Convective transport in nanofluids", J. Heat Transfer, 2006, 128, pp. 240 – 250.

[4]. Casson N., A flow equation for pigment oil suspensions of the printing ink type. In: Rheology of Sisperse Systems (C.C.Mill Ed.) Pergamon Press, Oxford, 1959,84-102.

[5]. Chen, H., Ding, Y., Tan, C., "Rheological behavior of nanofluids", New J Phys, vol. 9, 2007, pp. 367.

[6]. Choi, S. U. S. & Eastman, J. A. Enhancing thermal conductivity of fluids with nanoparticles: The Proceedings of the 1995 ASME InternationalMechanical Engineering Congress and Exposition, San Francisco, USA, ASME, FED 231/MD, 66, 99–105 (1995)

[7]. Deepak Sarve, Pradip Kumar Gaur, Vishnu Kumar Sarma : Numerical simulation for activation energy impact on Darch-Forchheimer flow of Casson fluid suspended with nano particles over a stretching cylinder. Science and Technology Asia, Vol.26, No.4 (2021), pp.107-115. *https://tci-thaijo.org/index.php/SciTechAsia, ISSN 2586-9000, E-ISSN 2586-9027*

[8]. Dogonchi AS, Heremet MA, Ganji DD, Pop I. Free convection of copper–water nanofluid in a porous gap between hot rectangular cylinder and cold circular cylinder under the effect of inclined magnetic field. J Therm Anal Calorim. 2019; 135(2):1171-84.

[9]. Duan, F., Kwek, D., Crivoi, A., "Viscosity affected by nanoparticle aggregation in Al2O3 – water nanofluids", Nanoscale Res Lett, vol. 6, 2011, pp. 248.

[10]. Elbashbeshy, E. M. A., Emam, T. G., El – Azab, M. S., Abdelgaber, K. M., "Laminar boundary layer flow along a stretching horizontal cylinder embedded in a porous medium in the presence of a heat source or sink with suction/injection", International Journal of Energy & Technology, 2012, 4 (28) pp. 1 – 6.
[11]. Fredrickson, A.G. "Principles and Applications of Rheology", Prentice –Hall, Englewood Cliffs, NJ, USA, 1964.
[12]. Gireesha B.J. Shankaralingappa B.M., Prasannakumarand B.C. Nagaraja B., MHD flow and melting heat transfer of dusty Casson fluid over a stretching sheet with CattaneoChristov heat flux model, International Journal of Ambient Energy, (2020), 1-22.
[13]. Ishak, A., Nazar,R., Pop,I., "Magnetohydrodynamic (MHD) flow and heat transfer due to a stretching cylinder", Energy Convers Manag , 2008, 49:pp. 3265 – 3269.
[14]. Kandasamy, R., Hayat, T. & Obaidat, S. Group theory transformation for Soret an Dufour effects on free convective heat and mass transfer with thermophoresis and chemical reaction over a porous stretching surface in the presence of heat source/sink. *Nuclear Engineering and Design.* **241**, 2155–2161 (2011).
[15]. Khan MI, Zaigham QM, Alsaedi A, Hayat T. Thermally stratifiedflow of second grade fluid with non-Fourier heat flux and temperature dependent thermal conductivity. Res Phys. 2018; 8:799-804.
[16]. Kulkarni, DP., Das, DK., Chukwu, GA., "Temperature dependent rheological property of copper oxide nanoparticles suspension (nanofluid)", J Nanosci Nanotechno, vol. 6,2006, pp. 1150.
[17]. Kumar K.G., Archana M., Gireesha B.J., Krishanamurthy M.R. and Rudraswamy N.G.,Cross diffusion effect on MHD mixed convection flow of nonlinear radiative heat and mass transfer of Casson fluid over a vertical plate. Results in Physics, 8, (2018), 694-701.
[18]. Kumar K.G., Gireesha B.J., Prasannakumara B. C., Ramesh G.K. and Makinde, Phenomenon of Radiation and Viscous Dissipation on CassonNanoliquid Flow Past O.D. A Moving Melting Surface. Diffusion Foundations, 11, (2017), 33-42.
[19]. Lin, C. R., and Shih, Y. P., "Buoyancy effects on the laminar boundary layer heat transfer along vertically moving cylinder", J. Chin. Inst. Eng., vol. 4, 1981, pp. 45 – 51.
[20]. Lin, C. R., and Shih, Y. P., "Laminar boundary layer heat transfer along static and moving cylinder", J. Chin. Inst. Eng., vol. 3, 1980, pp. 73 – 79.
[21]. Mahmoud MAA, MegahedAM. MHD flow and heat transfer characteristics in a Casson liquid film towards an unsteady stretching sheet with temperature-dependent thermal conductivity. Braz J Phys. 2017;47(5):512–23.
[22]. Malik., M. Y,Naseer M,Nadeem S, Rehman,A., "The boundary layer flow of Casson nanofluid over a vertical exponentially stretching cylinder", Appl Nanosci, 2013, 4:869–873.
[23]. Nagarani, P., Sarojamma, G., "Flow of a Casson fluid through a stenosed artery subject to periodic body acceleration", Proc. Of the 9th
[24]. Namburua, PK., Kulkarni, DP., Misrab, D., Das, DK., "Viscosity of copper oxide nanoparticles dispersed in ethylene glycol and water mixture", Exp Therm Fluid Sci, Vol. 32, 2007, pp. 397.
[25]. Patil PM, Kumbarwadi N, Aloor S. Effects of MHD mixed convectionwith non-uniform heat source/sink and cross-diffusion over exponentially stretching sheet. Int J Numer Methods Heat fluid Flow. 2018. https ://doi.org/10.1108/hff-04-2017-0149.
[26]. Penkavova, V., Tihon, J., Wein, O., "Stability and rheology of dilute tio2– water nanoflids, Nanoscale Res Lett", vol. 6, 2011, pp. 273.
[27]. Ramadevi B, Anantha Kumar K, Sugunamma V, Reddy JVR, Sandeep N. Magnetohydrodynamic mixed convective flow of micropolar fluid past a stretching surface using modified Fourier's heat flux model. J Thermal Anal Calorim. 2019. https://doi.org/10.1007/s1097 3-019-08477 -1.
[28]. Sadiq M.A. and Hayat T., Characterization of Marangoni Forced Convection in CassonNanoliquid Flow with Joule Heating and Irreversibility. Entropy, 22(4), (2020), 433.
[29]. Sarojamma G, Vendabai K, (2015) : Boundary Layer Flow of a Casson Nanofluid past a Vertical Exponentially Stretching Cylinder in the Presence of a Transverse Magnetic Field with Internal Heat Generation/Absorption, *World Academy of Science, Engineering and Technology, International Journal of Mathematical and Computational Sciences*, Vol:9, No:1, pp.138-143, ISNI:0000000091950263, doi.org/10.5281/zenodo.1099346

[30]. Sarojamma, G., Vishali, B., Ramana, B., "Flow of blood through a stenosed catheterized artery under the influence of a body acceleration modeling blood as a Casson fluid", Int. J. Of Appl. Math and Mech ,2012, 8(11): pp. 1 – 17.
[31]. Sheikholeslami, M. *et al*. Heat transfer simulation during charging of nanoparticle enhanced PCM within a channel. *Physica A: Statistical Mechanics and its Applications* **525**, 557–565 (2019).
[32]. Tamoor M., Waqas M., Ijaz Khan M., Alsaedi Ahmed, Hayat T., (2017): Magnetohydrodynamic flow of Casson fluid over a stretching cylinder, Results in Physics, Vol.No.7, pp.498-502, https://doi.org/10.1016/j.rinp.2017.01.005
[33]. Tawade J, Abel MS, Metri PG, Koti A. Thin film flow and heat transfer over an unsteady stretching sheet with thermal radiation, internal heating in the presence of external magnetic field. Int J AdvAppl Math Mech. 2016;3(4):29–40.
[34]. Wang, C. Y., "Fluid flow due to a stretching cylinder", Phys Fluids. , 1988, 31: pp. 466 – 468.
[35]. Wong, K. F. V. & Leon, O. D. Applications of nanofluids: current and future. *Adv. Mech. Engng*. 1–11 (2010).
[36]. WSEAS Int. Conf. On Mathematical and Computational Methods in Science and Engineering, Trinidad and Tobago, 2007, pp. 237 – 244.
[37]. Zuhra S, Khan NS, Khan MA, Islam S, Khan W, Bonyah E. Flow and heat transfer in water based liquid film fluids dispensed with graphene nanoparticles. Res Phys. 2018; 8:1143-57.

International Research Journal
IJNRD
Research Through Innovation